

The cure and diffusion of water in halogen containing epoxy/amine thermosets

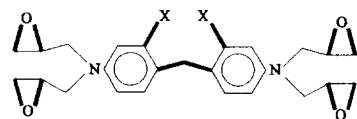
David Hayward, Elisabeth Hollins, Peter Johncock*, Iain McEwan, Richard A. Pethrick† and Elisabeth A. Pollock

Department of Pure and Applied Chemistry, Thomas Graham Building, 295 Cathedral Street, University of Strathclyde, Glasgow G1 1XL, UK and *Structural Materials Centre, Defence Research Agency, Farnborough, Hants GU14 6TD, UK
 (Received 2 February 1996; revised 27 May 1996)

Dielectric measurements were performed to determine the effect of chlorine, methyl and trifluoromethyl substituents on the cure of bis[*N,N*-bis(2,3-epoxypropyl)-4-aminophenyl]methane with 4,4'-diaminodiphenylsulfone and 4,4'-bis[1,4-phenylenebis(1-methylethylidene)]-bis[2,6-dimethyl]benzamine, and the data were analysed to give gelation and vitrification points. Infra-red measurements were also carried out during the cure process to monitor the consumption of epoxy groups. Dynamic mechanical thermal analysis and density measurements were carried out on the *N,N*-diglycidylaniline system and a reduction in the glass transition temperature was observed to occur with the incorporation of a trifluoromethyl group into the resin structure. Dielectric and gravimetric studies are reported on the absorption of water by these resins. In agreement with gravimetric data for water absorption, dielectric data obtained at 10 Hz showed that trifluoromethyl substitution increases the diffusion coefficient whereas chlorine substitution decreased it. The chlorinated resin exhibited a higher than expected initial dielectric increment, which has been attributed to the effect of a micro-porous surface structure of the resin. Atomic force microscopy of the resin surfaces indicates that the chlorinated and fluorinated resins have greater surface roughness than the protonated analogues, consistent with the dielectric observations. Analysis of the amount of 'bound' and 'free' water in the resin systems shows that the halogenated resins have a lower percentage of bound water and more of the water is in the 'free' state. © 1997 Elsevier Science Ltd. All rights reserved.

INTRODUCTION

Understanding the nature of the interaction of water with epoxy resins used in the fabrication of fibre reinforced composites is of considerable technological importance and has been the subject of a number of systematic investigations¹⁻⁸. Water ingress into composite structures can have both enhancing and detrimental effects. Initially water absorption leads to plasticization of the matrix without significant loss in rigidity, but is accompanied by an increase in the impact strength.

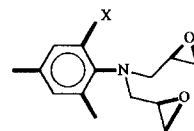


X = H, Cl, CF₃ or CH₃

However, increase in the level of water absorption will ultimately lead to a decrease in tensile modulus and loss of compressive strength, and possible detachment of resin from the carbon or glass fibre structure. Spectroscopic and dielectric studies indicate that water molecules interact with specific groups within these resins²⁻⁸. Introduction of halogen groups into an epoxy

resin reduces its affinity and rate of water adsorption⁹⁻¹⁴, the effect being greatest for fluorine containing resins. Sorption and desorption kinetics in many cases obey pseudo-Fickian type behaviour despite the obvious complexity of the process occurring.

In this paper the use of dielectric measurements to monitor cure and water absorption characteristics of a range of halogen and non-halogen containing epoxy resins are described. The epoxy resin systems chosen for investigation were as follows:



and X = H or CF₃

cured with diamines. This study aims to identify the factors which influence water absorption in thermoset resins and in particular the way in which water is distributed in the system.

EXPERIMENTAL

Materials

The base resin MY720 (Ciba Geigy) contained about

† To whom correspondence should be addressed

Table 1 Cure schedules

Resin system	Stoichiometry	PHR	Cure schedule	Residual epoxy (%)
DGA/ <i>m</i> -DAB	100	26.3	17 h at 80°C and 6 h at 160°C	85 2.1
TFMDGA/ <i>m</i> -DAB	100	19.8	17 h at 80°C and 6 h at 160°C	14 0.2
TGDDM/DDS	60		1 h at 150°C and 5 h at 180°C	
Cl-TGDDM/DDS	60		1 h at 150°C and 5 h at 180°C	
CF ₃ -TGDDM/DDS	60		1 h at 150°C and 5 h at 180°C	

70% TGDDM by peak areas using reverse phase h.p.l.c. and had a 92% epoxy group content on which stoichiometric ratios are based. The epoxy group content of 92% indicates that some of the resin is not correctly functionalized and there are fewer epoxy groups than in the ideal structure. The preparation of the chloro-, trifluoromethyl- and methyl-substituted resins has been reported¹⁴, and the resins employed contained, by h.p.l.c., 70–75% of the respective epoxy compounds bis[2-chloro-*N,N*-bis(2,3-epoxypropyl)-4-aminophenyl]methane (Cl-TGDDM), bis[2-trifluoromethyl-*N,N*-bis(2,3-epoxypropyl)-4-aminophenyl]methane (CF₃-TGDDM) and bis[2-methyl-*N,N*-bis(2,3-epoxypropyl)-4-aminophenyl]methane (CH₃-TGDDM). Analysis of the halogenated systems for epoxy content using a variety of approaches¹⁵, unlike that of MY720, gave very inconsistent results and a similar epoxy content to that of MY720 was assumed. *N,N*-Bis(2,3-epoxypropyl)aniline (DGA) was prepared by the procedure described by Haydn and Balzejak¹⁶, and *N,N*-bis(2,3-epoxypropyl)-3-trifluoromethylaniline (TFMDGA) by a procedure used to prepare *N,N*-bis(2,3-epoxypropyl)trihaloanilines described by Herbert¹⁷. Distilled fractions of these epoxies were >99% pure by h.p.l.c. The curing agents used were 4,4'-diaminodiphenylmethane (DDS) (Ciba Geigy HT976), 4,4'-bis[1,4-phenylenebis(1-methylethylidene)]bis(2,6-dimethyl)benzamine (HPT1062) and 1,3-benzenediamine (*m*-DAB) (Aldrich). The structures of these molecules are shown in Scheme 1.

All measurements were taken in solutions or on films which were prepared from homogeneous mixtures prepared at 403 K *in vacuo*. For MY720 and its substituted derivatives a 60% stoichiometric ratio of DDS or HPT1062 was used. For DGA and TFMDGA a 100% stoichiometric ratio of *m*-DAB was used.

Low frequency dielectric measurements

Dielectric measurements were carried out during the cure of the resins, from 10⁻² to 10⁵ Hz, using a dielectric spectrometer which has been described previously¹⁸. The mixture of epoxy and hardener was placed in a liquid cell constructed from two electrodes separated by a fibre glass spacer of thickness 2 mm. Thin films of ~0.025 cm thickness were prepared for dielectric diffusion studies by placing the epoxy resin mixture between clamped glass plates, which had been pretreated with silicone release agent and were separated by glass fibre reinforced Teflon shims. The films were cured at a temperature of 423 K. The resin sheets were covered by a 100 Å layer of evaporated silver which forms a semi-permeable electrode. The cell structure was then encased in silicone sealant with only one

face of the cell being exposed to water. The samples were then immersed in deionized water at 298 K and the dielectric response measured at set intervals over the frequency range 10⁻²–10⁵ Hz¹⁸. After the first 18 h of measurement the change in dielectric response was slow enough to allow measurements to be extended to 10⁻³ Hz.

High frequency dielectric measurements

Films were prepared for high frequency dielectric measurements as for low frequency measurements with the samples being circular with a diameter of approximately 17 mm. Silver electrodes are evaporated on to both sides of the sample, and the polymer film takes the form of a membrane which bridges the end of a coaxial line. The sample is also connected to a water condenser assembly which is maintained at a temperature of 298 K. Measurements are performed over the frequency range 300 kHz–3 GHz using a Hewlett-Packard 8753A network analyser. The system is operated in reflection mode and corrections are made for the mismatches between the measurement cell and connector cable to the network analyser.

Infra-red measurements

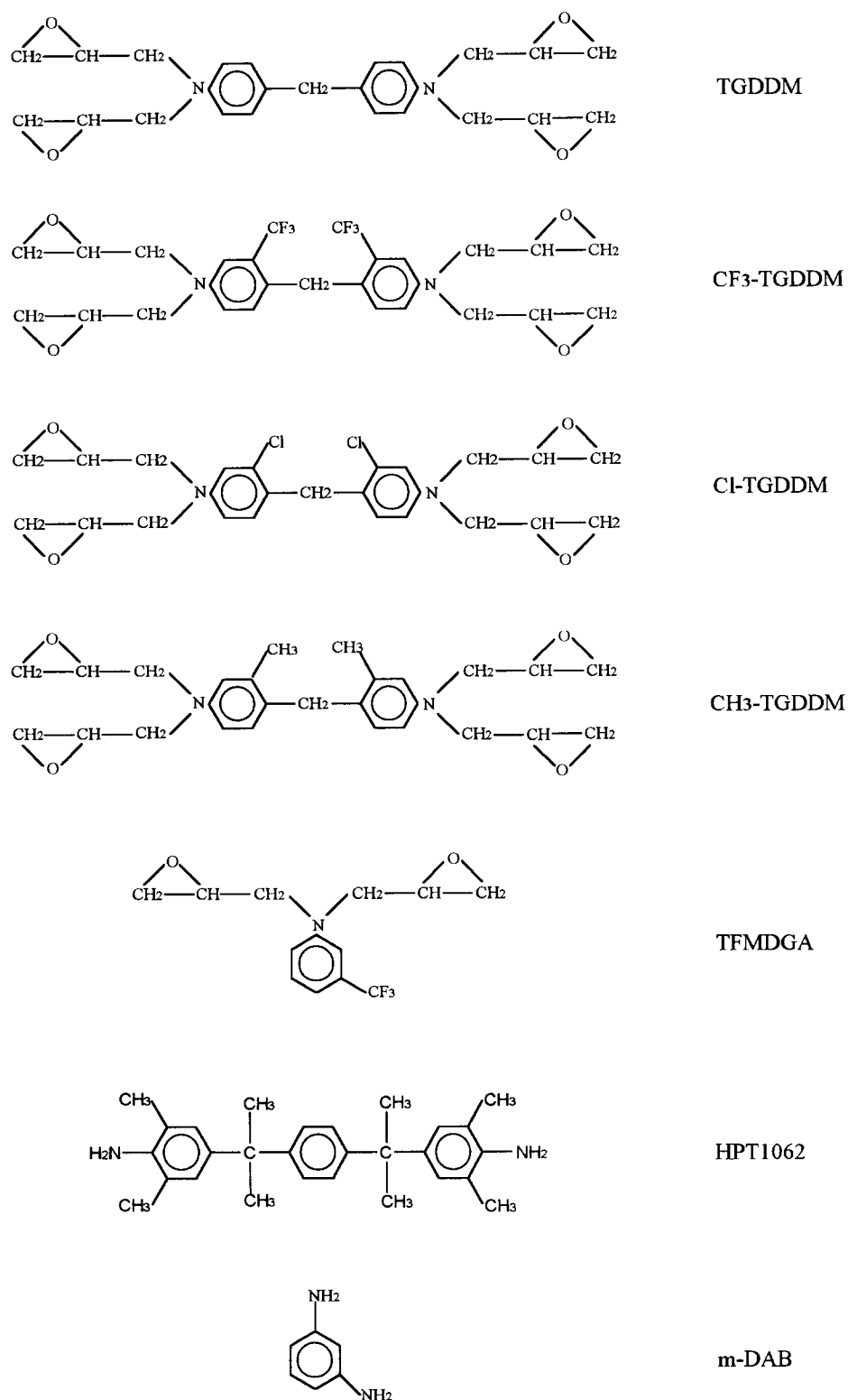
Infra-red (i.r.) spectra were obtained using a Nicolet 20-SXB FT i.r. spectrometer. Degassed resin and hardener mixtures were pressed between two preheated KBr discs and the spectral changes during cure recorded (Table 1).

Gravimetric measurements

Thin films of ~0.025 cm thickness were used to measure the weight gain due to water uptake as a function of time. Samples were immersed in deionized water at 298 K and weighed periodically using a Mettler M5 balance with a precision of better than 0.1%. The samples were removed from the water, wiped to remove excess of water and after 4 min the samples were weighed and reimmersed after 5 min total time out of water.

Dynamic mechanical thermal analysis (d.m.t.a.)

The Polymer Laboratories Dynamic Mechanical Thermal Analyser was used to test the mechanical properties of epoxy samples. Measurements were taken at a frequency of 10 Hz and a strain of ×1 while the temperature was scanned at 5 K min⁻¹ from a starting temperature of 318 K until well after the glass transition temperature. The samples for testing were prepared with dimensions of 20 mm × 10 mm × 0.5 mm and were subjected to a forced oscillation using a single cantilever mode of action.



Scheme 1

Sample densities

The densities of the epoxy samples were calculated at 295 K by using a standard gravity bottle.

RESULTS AND DISCUSSION

Cure studies

In order that the moisture diffusion measurements were carried out on fully cured resins it was necessary

to determine the correct cure cycle for the resin. The recommended cure cycles provided by manufacturers does not always lead to complete cure and, in this study, measurements are also reported on non-commercial resins for which no cure data exist. Two parameters are important in determining cure: the change of mobility of the resin with time and degree of conversion. The utility of dielectric measurements for the investigation of cure has been discussed¹⁹⁻²³ and application of a variant of this approach is presented in this paper.

Measurements were performed on samples cured isothermally at 423 K for the TGDDM based system cured with DDS and HPT1062 over the frequency range 10^{-3} – 10^5 Hz. Three-dimensional plots of the dielectric permittivity and loss of the TGDDM/DDS samples are shown in *Figure 1*. Since all of the dielectric permittivity and loss plots are similar only the plots for TGDDM/DDS are shown. All of the permittivity and loss plots against frequency and time exhibit three distinct relaxation features. At low frequency and short times, a large dielectric loss is observed, which rapidly decreases as cure proceeds and is attributed to the blocking electrode

effects²⁴. A high level of d.c. conductivity, characterized by an approximately ω^{-1} slope, is observed initially, which is dramatically reduced during cure. However, in many of the samples a significant d.c. conductivity is still clearly evident in the fully cured matrix. The d.c. conductivity in epoxy resins can be ascribed to chloride residues left from the synthesis of the oxirane ring structure. In the liquid resin these ions will have a very high mobility, which is reduced as the molecular weight and hence viscosity of the media are increased by reaction. The generation of a three-dimensional network will be expected to inhibit the ionic conductivity of

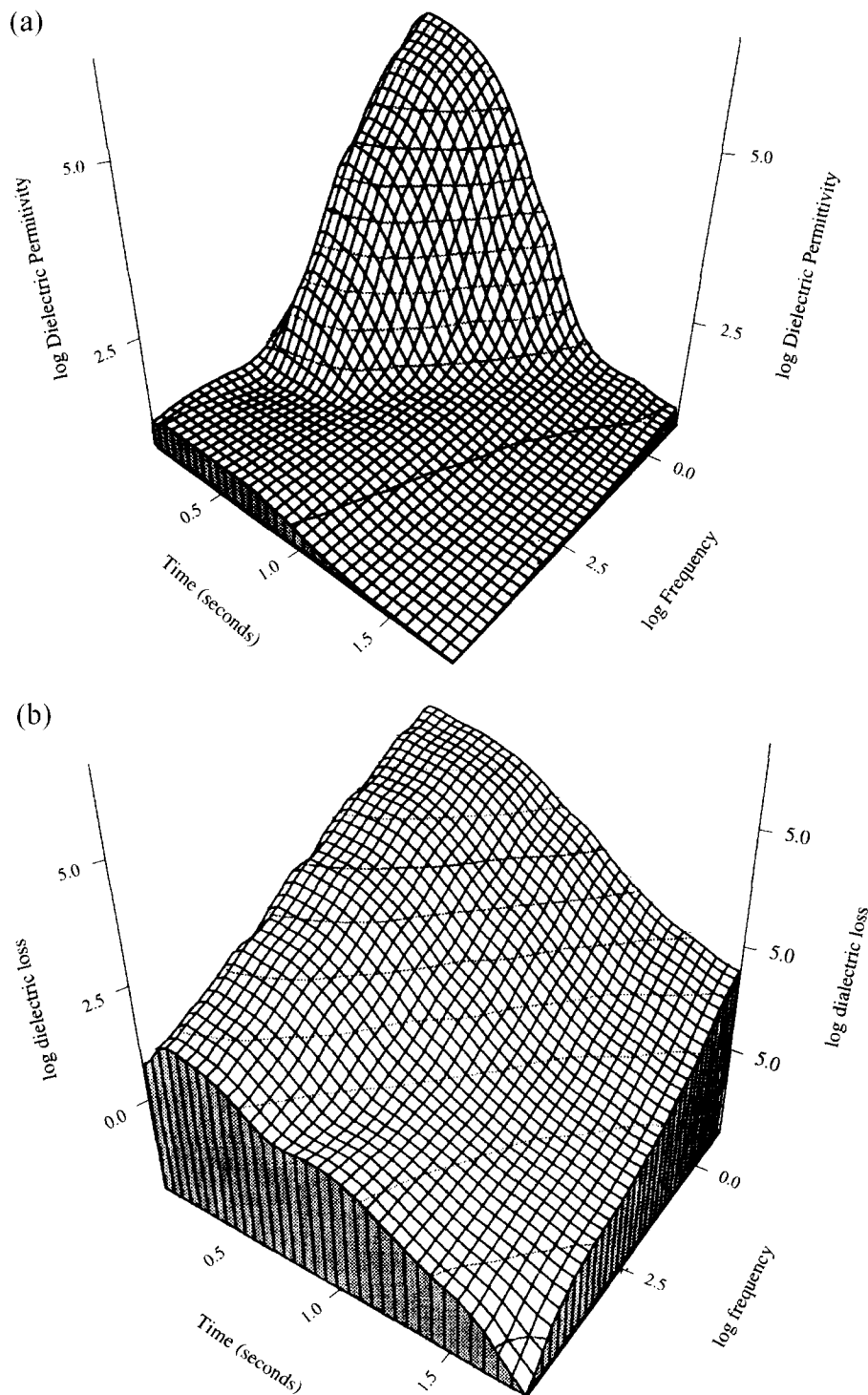


Figure 1 (a) Dielectric permittivity and (b) dielectric loss for cure of TGDDM/DDS

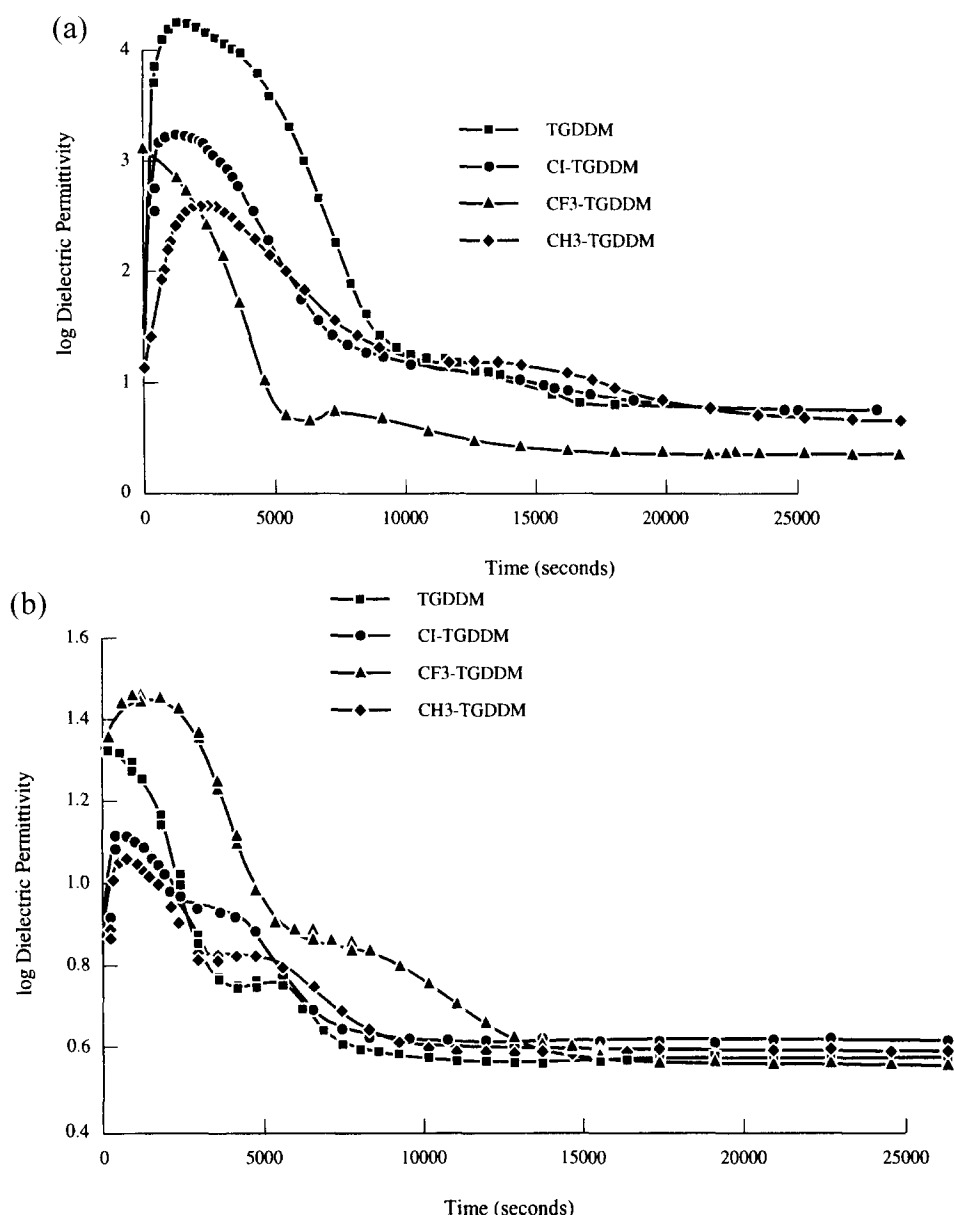


Figure 2 Dielectric permittivity at 10 Hz for (a) DDS cured resin systems, and (b) HPT1060 cured resin systems

the media and hence the disappearance of this low frequency peak may be associated with the gelation process.

For these samples there was insufficient material to confirm the gel time with another technique; however, a previous experiment using the same technique has shown a broad correlation between the mobility of the ions and the gel point. The dipolar relaxation which dominates the high frequency region and is observed as a peak in the loss spectrum disappears after approximately 100 min. Loss of this main dipolar relaxation process is associated with vitrification of the resin. Vitrification, the point at which dipolar reorientation ceases, can be determined by plotting the dielectric permittivity as a function of time at a frequency of 10 Hz, as shown in Figure 2. The features observed are respectively associated with gelation and vitrification in the system. The gelation and vitrification times are presented in Table 2.

I.r. measurements

I.r. measurements were carried out on the DGA based systems cured with *m*-DAB in order to establish the extent of conversion during the cure cycle. The DDS systems were initially cured at 423 K for 1 h and then for 5 h at 450 K, whereas the *m*-DAB systems were cured at 353 K for 17 h and then for 6 h at 433 K. The i.r. measurements were carried out after each stage of the cure schedule. The DGA resin contained five adjacent aromatic hydrogens, which absorbed strongly in the region below 800 cm^{-1} and gave two bands in regions $770\text{--}730$ and $720\text{--}680\text{ cm}^{-1}$. The aromatic hydrogens of the *meta*-substituted TFMDGA resin absorbed in the region $800\text{--}750\text{ cm}^{-1}$. The cure process with DDS gave low residual epoxide values of between 1 and 2% on completion of the cure cycle. The initial spectra for the cure of DGA/*m*-DAB and TFMDGA/*m*-DAB both showed a strong epoxide ring absorption at 916 cm^{-1} and

Table 2 Gelation and vitrification times

Resin system	Time to gelation (s)	Time to vitrification (s)
TGDDM/DDS	9000	20 000
Cl-TGDDM/DDS	8000	19 000
CF ₃ -TGDDM/DDS	5000	18 000
CH ₃ -TGDDM/DDS	9000	22 000
TGDDM/HPT1060	3000	10 000
Cl-TGDDM/HPT1060	3000	12 000
CF ₃ -TGDDM/HPT1060	5500	19 000
CH ₃ -TGDDM/HPT1060	3000	12 000

reference bands at 1500 cm⁻¹. The intensities of the 916 cm⁻¹ absorptions were obtained using the FTi.r. integration software. Manual determination of the baseline correction was necessary because of the close proximity of other absorptions in this region. To allow for path length differences between samples, the peak intensities were ratioed to a common C–H reference absorption peak. The integrated intensity ratio of the initial spectrum was assigned a value of 100% and the percentage of the functional group remaining was calculated by comparing the integrated intensity ratio to that of the initial spectrum.

The variation of the epoxy content with cure conditions is summarized in *Table 1*. It was found that in all cases the residual epoxy content was related to the final post-cure temperature. The reference bands were subject to some small changes in breadth during the cure, but this did not affect the overall accuracy of the measurements reported. When the cure temperature was increased to 433 K the residual epoxide values decreased rapidly and gave final results of 2.1 and 0.2%. A pseudo-equilibrium had been reached at the initial cure temperature and it was only when the temperature of cure was increased that further reduction in the epoxy content was observed. The network formed initially is sufficiently restrictive to inhibit reaction, but with increase in mobility accompanying further heating the reaction can once more proceed. Cure is not completed until the sample has been heated to a temperature of 433 K for these systems.

D.m.t.a. measurements

An important characteristic of a thermoset resin is its glass–rubber transition temperature, T_g . The d.m.t.a. measurements were used to determine T_g and the results for the DGA based system, *Table 3*, indicate a slight lowering of the T_g of the resin with incorporation of the trifluoromethyl group. The drop in T_g from 429 K to 426 K with incorporation of fluorine indicates that there is either slightly more free volume and/or lower polymer–polymer interactions in the fluorinated system.

Density measurements

The extent of polymer–polymer packing is reflected in the density of a cured resin. Introduction of fluorine

would be expected to increase the density as was observed for the DGA based resin (*Table 3*), which shows a decrease from 1.33 to 1.27 g cm⁻³ with the addition of fluorine. However, previous positron measurements on these systems²⁵ showed that the fluorinated resin contained an increased free volume at molecular level.

Water absorption studies

A critical parameter in the selection of a thermoset resin for composite and related applications is its susceptibility to moisture absorption. Two approaches are adopted in this paper for the quantification of water absorption: gravimetric measurements, which allow determination of the total water absorption, and associated diffusion coefficients and dielectric measurements, which additionally provide information on the nature of the environment in which the water molecules are located.

Gravimetric water uptake measurements

Measurements were performed on certain of the samples in this study. Although the sorption processes of liquids and vapour in glassy polymers follow complex mechanisms, water diffusion in epoxy resin matrices has been frequently represented by a Fickian behaviour^{26–28}. The features of Fickian diffusion have been described by Fujita²⁹:

- (i) The sorption curves are linear in the initial stages.
- (ii) Above the linear portion both absorption and desorption curves are concave to the abscissa. For absorption the linear region extends to over 60% or more of the region studied.
- (iii) When a series of reduced absorption curves are plotted for films of different thickness the curves are superimposable.

If a plane polymer sheet is exposed to a fluid, the change in the concentration (C) of a diffusing substance as a function of time (t) and position (x) is given by Fick's second law²⁸:

$$\frac{\partial C}{\partial t} = D \frac{\partial^2 C}{\partial x^2} \quad (1)$$

Table 3 D.m.t.a. and density results

Resin system	Final cure temperature (°C)	T_g (K)	E_a (kJ mol ⁻¹)	Density (g cm ⁻³)
DGA/ <i>m</i> -DAB	160	429	61.3	1.72
TFMDGA/ <i>m</i> -DAB	160	426	50.3	1.33

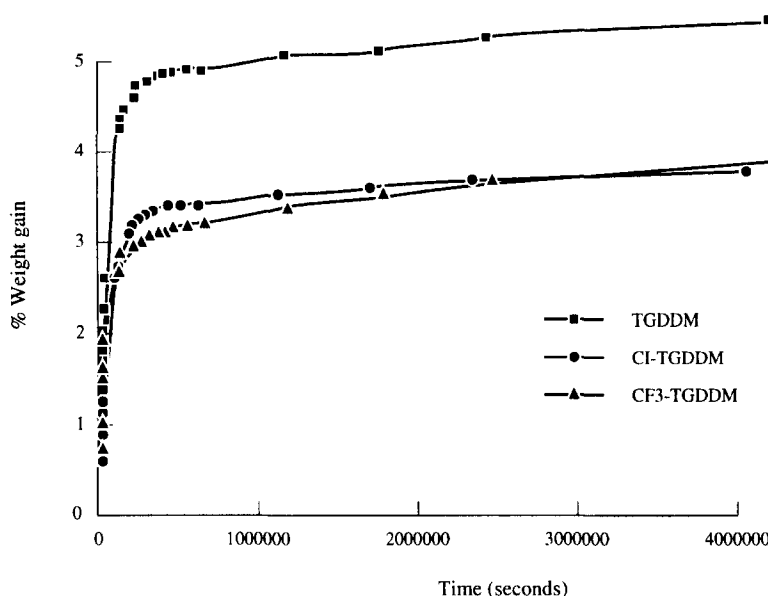
Table 4 Diffusion coefficients

Resin system	Gravimetric diffusion coefficient ($D \times 10^{10} \text{ cm}^2 \text{ s}^{-1}$)	Dielectric diffusion coefficient ($D \times 10^{10} \text{ cm}^2 \text{ s}^{-1}$)
TGDDM/DDS	15.6	14.2
Cl-TGDDM/DDS	3.0	8.3
CF ₃ -TGDDM/DDS	17.7	16.8
DGA/ <i>m</i> -DAB	—	7.4
TFMDGA/ <i>m</i> -DAB	—	19.6

halogen containing resins did not adsorb as much water. The diffusion coefficients given in *Table 4* are in fair agreement with published values³⁰ and confirm that substitution of chloride decreases, whereas the introduction of trifluoromethyl groups increases the diffusion coefficient.

Dielectric measurements

Measurements were performed over the frequency

**Figure 3** Gravimetric determination of water sorption for DDS cured system

where D is the diffusion coefficient. If the material has a uniform initial diffusant concentration (C_0) and the surface is kept at a constant concentration C_{\max} , the solution of equation (1) is²⁷

$$\frac{C - C_0}{C_{\max} - C_0} = 1 - \frac{4}{\pi} \sum_{n=0}^{\infty} \frac{(-1)^n}{2n+1} \exp[-D(2n+1)^2 \pi^2 t/h^2] \times \cos \frac{(2n+1)\pi x}{h} \quad (2)$$

The total amount of substance diffusing in the polymeric material (M) as a function of time is given by the integral of equation (2) across the thickness (h):

$$\frac{M}{M_{\max}} = 1 - \frac{8}{\pi^2} \sum_{n=0}^{\infty} \frac{1}{(2n+1)^2} \exp[-D(2n+1)^2 \pi^2 t/h^2] \quad (3)$$

where M_{\max} is the maximum quantity of the diffusing substance at infinite time. A simplified form of equation (4) for values of M/M_{\max} lower than 0.6²⁸ has the form:

$$\frac{M}{M_{\max}} = \frac{4}{h\sqrt{\pi}} \sqrt{Dt} \quad (4)$$

For gravimetric analysis equation (4) is a valid representation of the time dependence of the water uptake, and the results for the systems investigated are presented in *Table 4* and *Figure 3*. The gravimetric water uptake for the TGDDM system was of the order of 5.5% with the water uptake in the fluorinated and chlorinated resin being of the order of 3.5%, showing that the

range 10^{-3} – 3×10^9 Hz over a period of two weeks of water immersion. The data indicate a rapid increase in the dielectric permittivity and loss (*Figure 4*), which becomes constant after a period of time. The dielectric relaxation spectra can be subdivided into three regions:

(i) Below 10 Hz the loss observed is associated with a combination of processes associated with the heterogeneous nature of the epoxy resin and the tail of the glass transition process. The ingress of the water leads to a shift of the glass transition to lower temperatures and is reflected in a shift of the dielectric loss to higher frequency. A shift of the loss to higher and then to lower frequency is consistent with the T_g process moving to lower temperature and then increasing again. Lowering of the T_g can also allow densification of the matrix with a subsequent rise in T_g and a shift of the dielectric loss to lower frequencies. The ripples in the dielectric traces reflect changes in the structure occurring during the water sorption process. These features are real and relate to stress relaxation within the systems. Further investigation would be required to determine the processes taking place.

(ii) The weak relaxation feature at approximately 10 kHz is associated with reorientation of the hydroxyl group, generated from opening of the epoxy ring by attack of the amine. Increase in its amplitude on absorption of water suggests that molecules of water are being bound to the OH dipole and increase the relaxation strength. Analysis of the change in the relaxation strength on hydration allows calculation of the increment $\Delta\epsilon'$ (bound) (*Table 5*). These water molecules have a

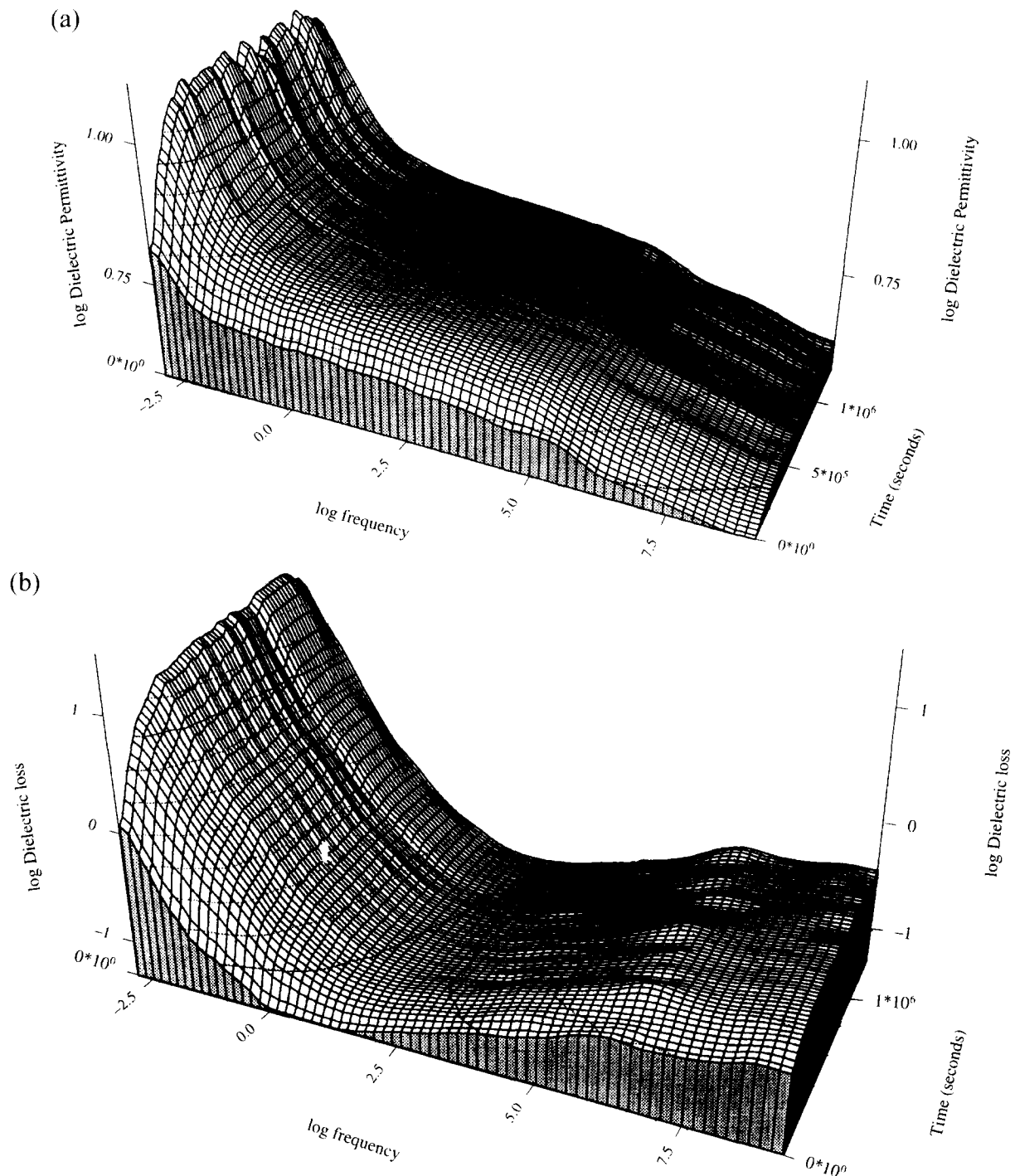


Figure 4 (a) Dielectric permittivity for TGDDM/DDS; (b) dielectric loss for TGDDM/DDS; (c) dielectric permittivity for Cl-TGDDM/DDS; (d) dielectric loss for Cl-TGDDM/DDS; (e) dielectric permittivity for CF₃-TGDDM/DDS; (f) dielectric loss for CF₃-TGDDM/DDS; (g) dielectric permittivity for DGA/*m*-DAB; (h) dielectric loss for DGA/*m*-DAB; (i) dielectric permittivity for TFMDGA/*m*-DAB; (j) dielectric loss for TFMDGA/*m*-DAB; (k) high frequency dielectric permittivity for DGA/*m*-DAB; (l) high frequency dielectric loss for DGA/*m*-DAB; (m) high frequency dielectric permittivity for TFMDGA/*m*-DAB; (n) high frequency dielectric loss for TFMDGA/*m*-DAB; (o) high frequency dielectric permittivity for DGA/*m*-DAB (second sorption after drying); (p) high frequency dielectric loss for DGA/*m*-DAB (second sorption after drying); (q) high frequency dielectric permittivity for TFMDGA/*m*-DAB (second sorption after drying); (r) high frequency dielectric loss for TFMDGA/*m*-DAB (second sorption after drying)

Table 5 Percentage bound and free water

Resin system	$\Delta\epsilon'$ (total)	$\Delta\epsilon'$ (bound)	Percentage bound	$\Delta\epsilon'$ (free)	Percentage free
TGDDM	1.514	0.276	18	1.238	82
Cl-TGDDM	1.137	0.127	11	1.010	89
CF ₃ -TGDDM	0.881	0.106	12	0.775	88
DGA	1.5	0.3	20	1.2	80
TFMDGA	0.8	0.1	12	0.7	88

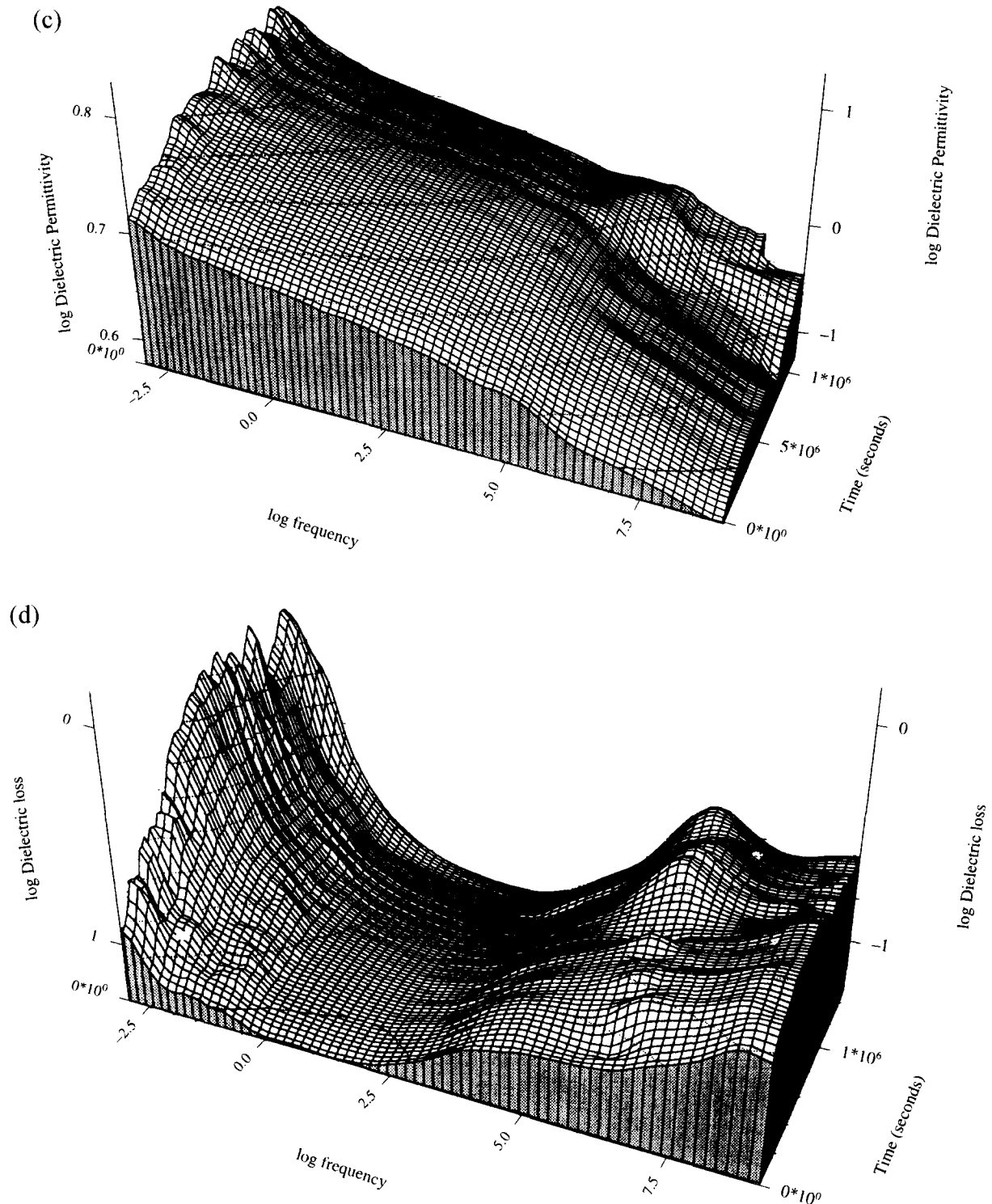


Figure 4 (Continued)

relaxation frequency which is being controlled by the intramolecular potential of the hydroxyl group rather than that of the molecules' molar mass as would be the case if they were freely dispersed in the matrix. It can be seen in *Figure 4* that the water molecules distribute themselves throughout the region 10^6 – 10^9 Hz. However, there is sufficient separation between the process at 10^4 Hz and that at 10^9 Hz to attempt to ascribe these to different types of environment.

(iii) The relaxation above 10^9 Hz is associated with 'free' water; the dipole relaxation of water occurring

at room temperature at 2×10^{10} Hz. The occurrence of processes in this frequency range in a solid is indicative of molecules clustering within microvoids within the epoxy resin matrix.

Quantitative interpretation of the dielectric measurements requires an extension of the theory used for gravimetric analysis. The cell used for the dielectric study allows diffusion from one side only, the edges and reverse side being sealed with silicone rubber and a copper electrode, respectively. The gravimetric theory involves the mass of water molecules whereas the dielectric

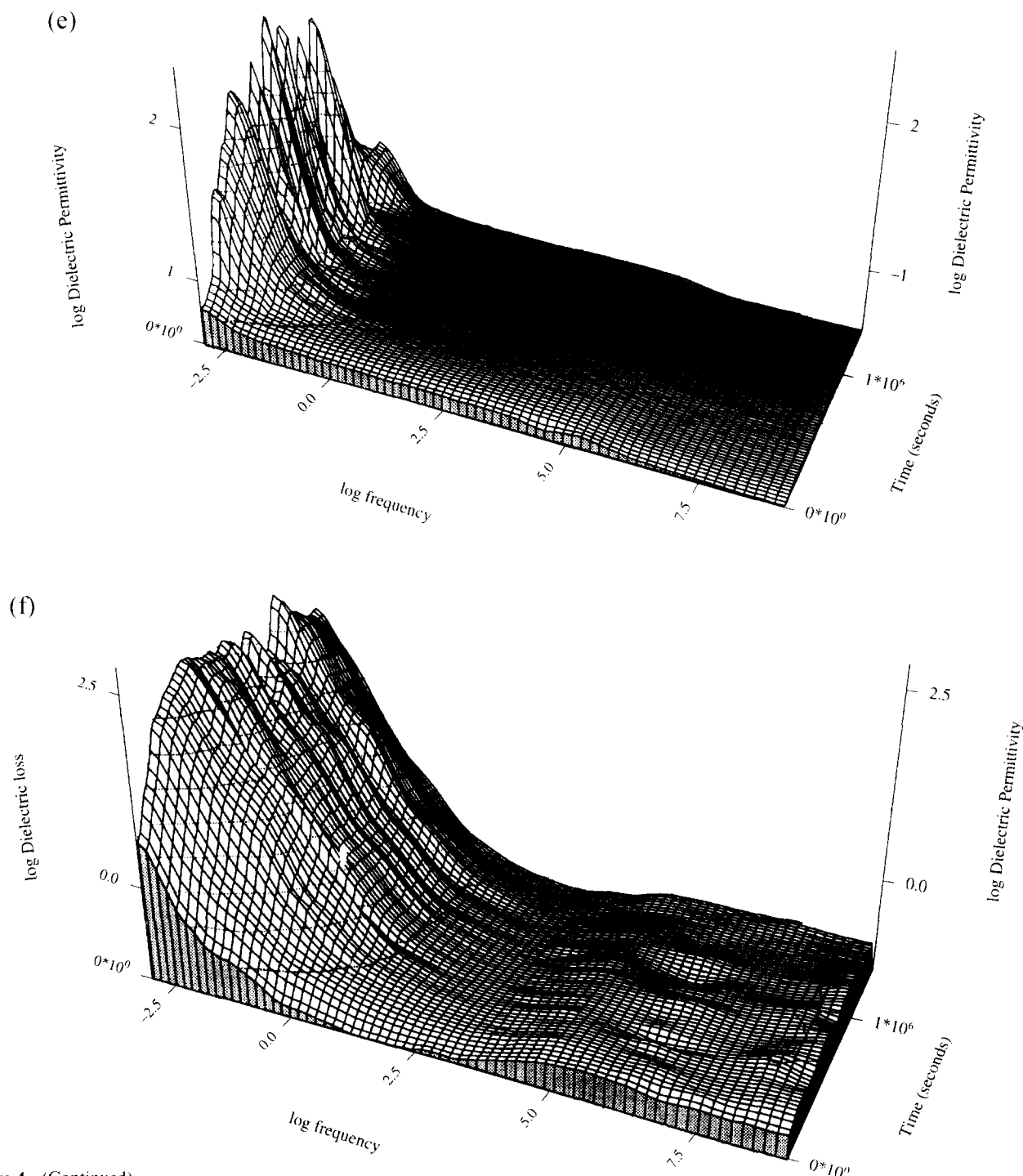


Figure 4 (Continued)

experiment measures the change in the permittivity of the media. Under isothermal conditions the increase in the permittivity observed during water diffusion ($\epsilon' - \epsilon'_0$) is proportional to the number of water dipoles present in the system^{31,32}. Therefore, a linear relationship between ϵ' and water concentration in the polymer is expected. It has, however, been pointed out previously^{27,31,33} that there is a discrepancy between the observed increment and that predicted on the basis of the amount of water absorbed. The permittivity of free water is 80.4 at 293 K³¹⁻³⁴ and water molecules may be assumed to be either clustered, in which case the dielectric increment should closely correlate with the value for water, or be bound to the matrix, in which case a lower value may

be expected. In the case of the dielectric analysis the diffusion can be modelled according to the following equation:

$$\frac{\epsilon' - \epsilon'_0}{\epsilon'_{\max} - \epsilon'_0} = 1 - \frac{4}{\pi} \sum_{n=0}^{\infty} \frac{(-1)^n}{2n+1} \exp[-D(2n+1)^2\pi^2 t/h^2] \quad (5)$$

where ϵ'_{\max} is the maximum value of the dielectric permittivity achieved by the water diffusing into the polymer matrix. In this case the diffusion coefficient (D) can be estimated by considering only the first term in equation (5) (i.e. $n = 0$) and using the half time ($t_{1/2}$) corresponding to $\epsilon' - \epsilon'_0 / \epsilon'_{\max} - \epsilon'_0$, with the condition that

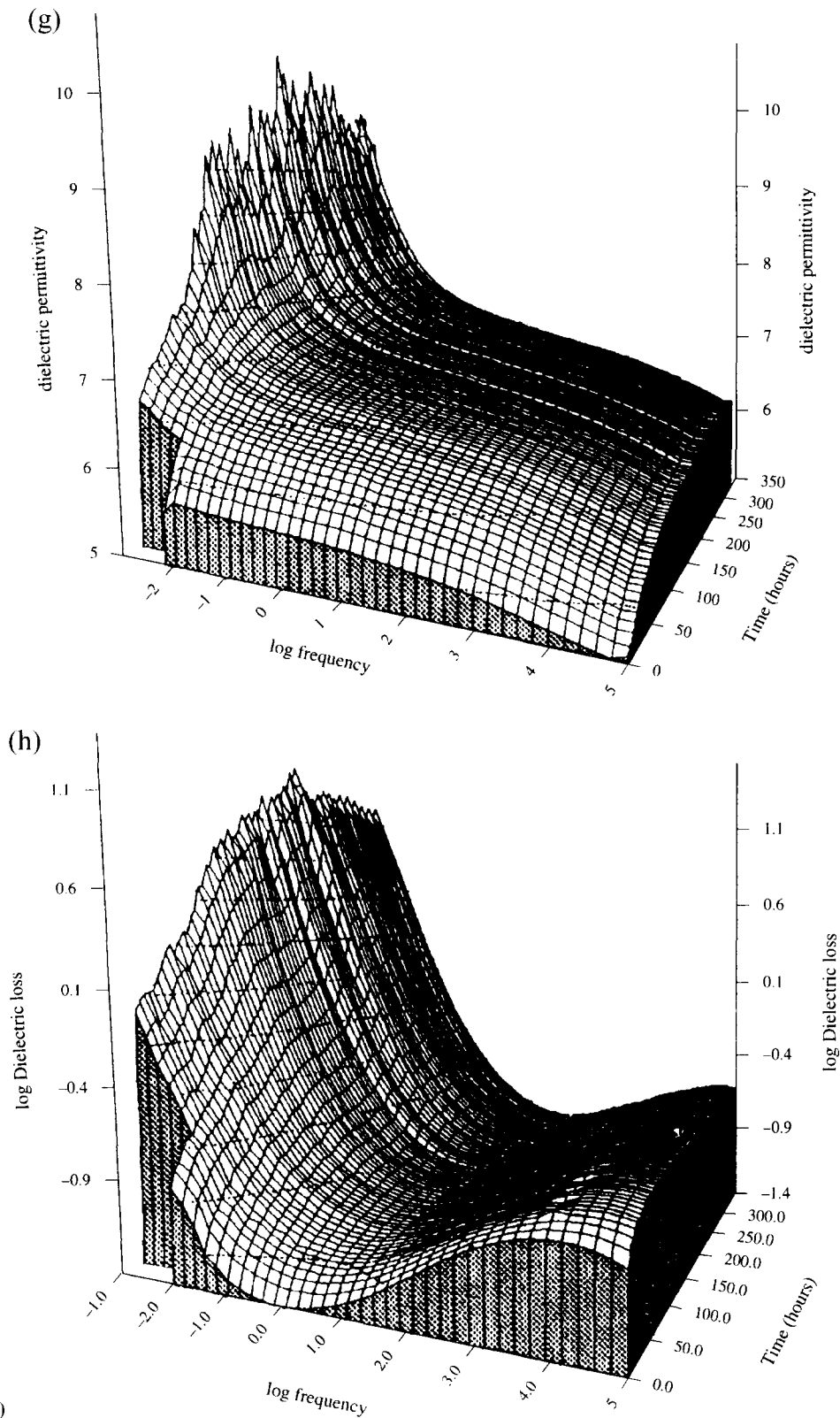


Figure 4 (Continued)

$\exp[-D\pi^2 t_{1/2} h^2] < 1$. Thus,

$$D = -\frac{h^2}{t_{1/2}\pi^2} \ln\left[\frac{\pi}{8}\right] \quad (6)$$

Furthermore, equation (6) can be written in the approximate form:

$$D = 0.0947h^2/t_{1/2} \quad (7)$$

It has been previously observed that measurements of the diffusion permittivity at different frequencies leads to different values of the apparent diffusion coefficient³⁵, lower apparent values being observed at higher frequencies. It is assumed that the variation of the dielectric permittivity measured at 10 Hz (Figure 5) reflects the total relaxation spectrum of the water molecules in the matrix and hence is correlated with the total sorption process measured gravimetrically. Measurements at about 10^6 Hz

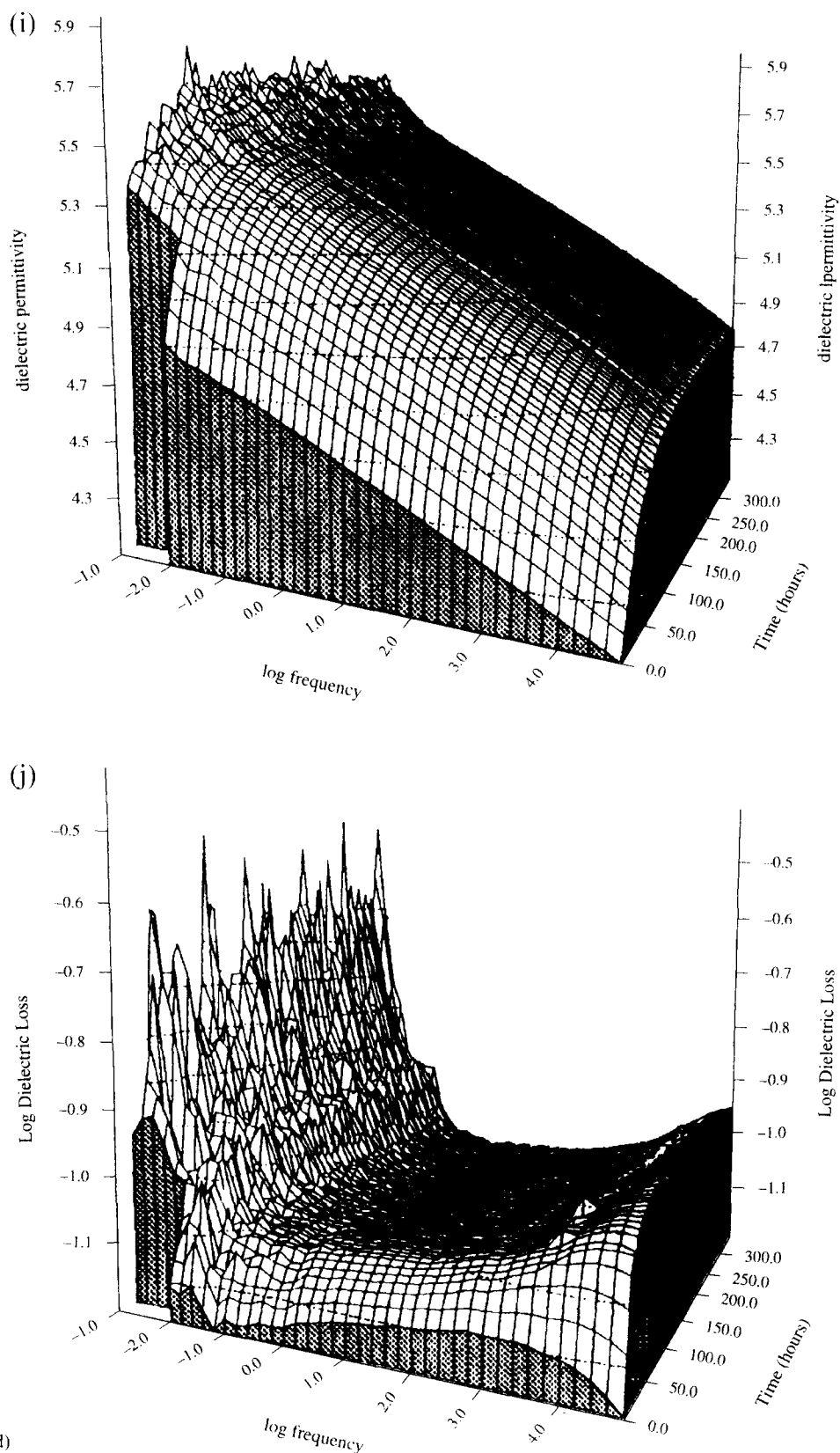


Figure 4 (Continued)

will reflect only water molecules which are able to move more easily in the matrix and are designated 'free' water.

Dielectric results indicate that the chlorinated and fluorinated resins adsorb less water than the base resin, but with the fluorinated resin adsorbing less water than the chlorinated resin. However, careful analysis of the observed changes indicates that the dielectric

measurements can be subject to the effects of a contribution due to interfacial polarization as a consequence of a porous structure next to the top electrode. Previous investigations have confirmed this effect in the case of thermoplastic modified epoxy resins³⁶. The surface micropores are quickly filled with water, and a liquid cell which is similar to the blocking electrode

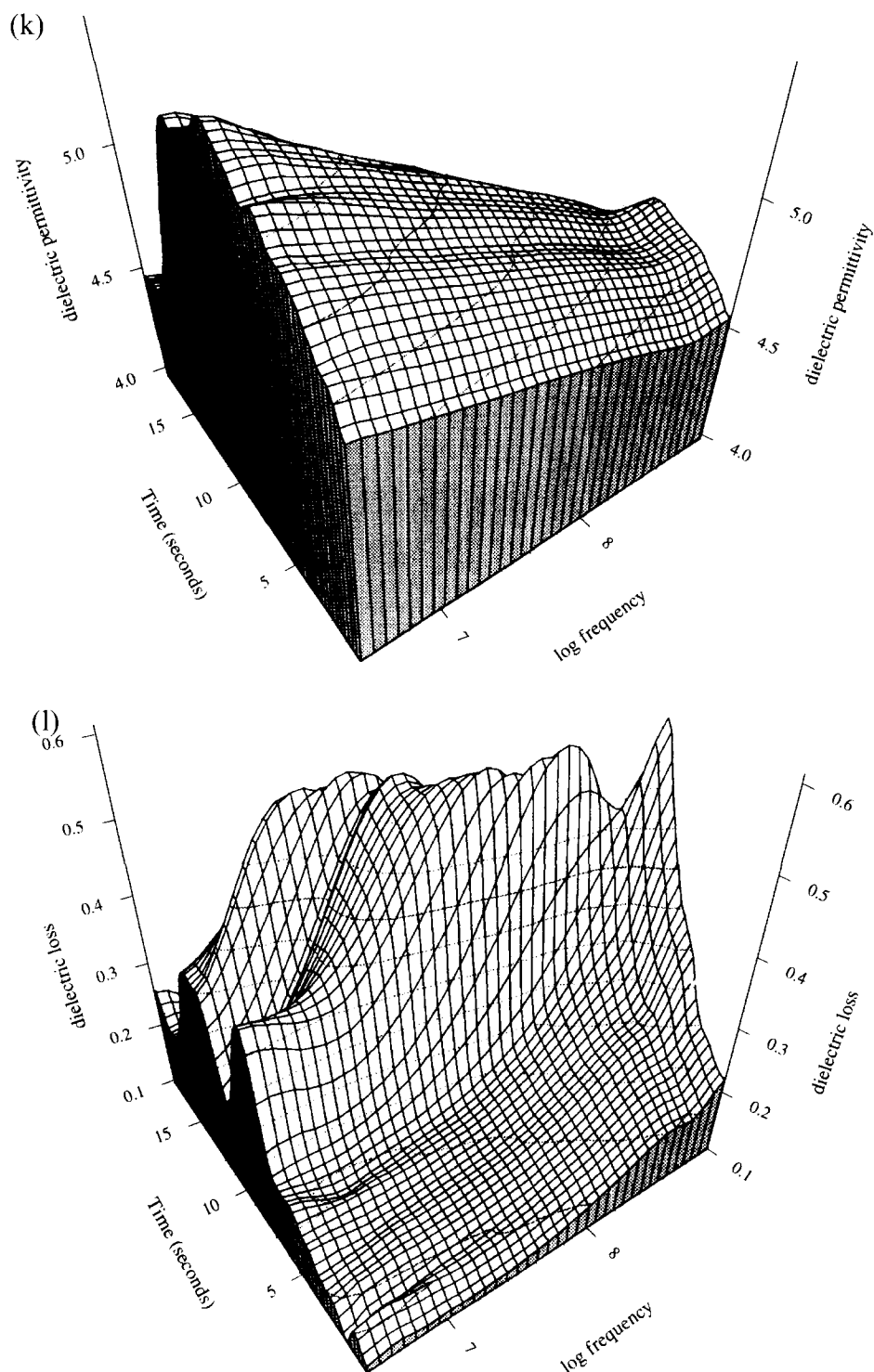


Figure 4 (Continued)

phenomenon, illustrated in the cure process, adds to the dielectric increment. Once the diffusion process has been allowed to settle down the effects of these surface anomalies are lost and the change in the dielectric profile with time reflects the uptake of moisture by the bulk resin. The value of the dielectric permittivity for these materials stays higher than those for the other materials and as a consequence a final higher value of the equilibrium value is observed. This phenomenon explains the apparent differences between the gravimetric and dielectric data reported in *Figures 3 and 5*. In the

gravimetric experiment, water in the microporous surface region has a negligible effect on the weight, but a major effect on the dielectric permittivity data. The calculated diffusion coefficients (*Table 4*) for both dielectric and gravimetric results correlated reasonably well, the uncertainty in the former being high because of the problem of the initial data being influenced markedly by the effects of microvoids. Both sets of results showed that the diffusion coefficient for the chlorinated system was significantly smaller than those of the fluorinated samples, and the base resin showed that water

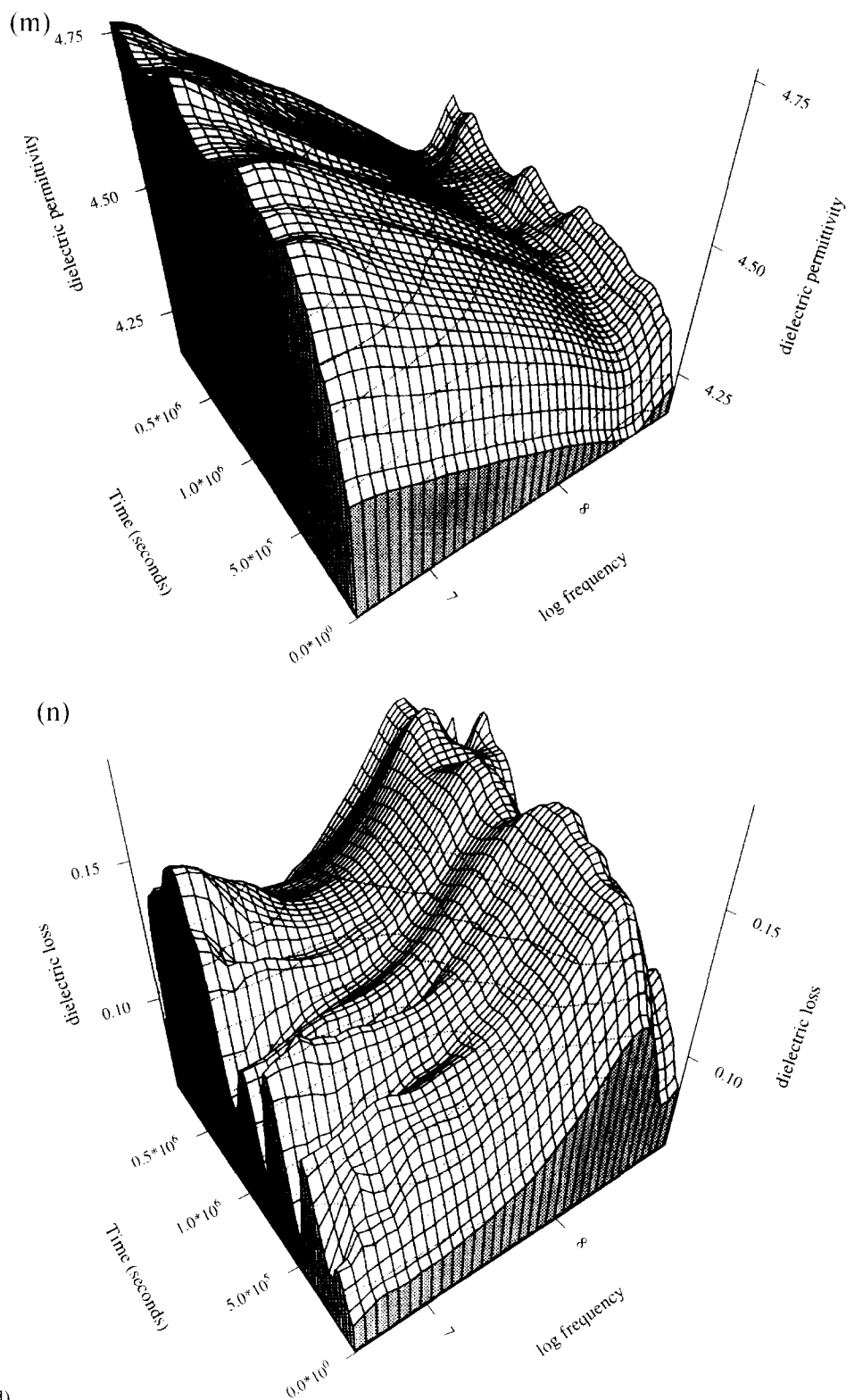


Figure 4 (Continued)

adsorption was slower for the chlorinated system. Calculation of the water distribution in the system indicates that the percentage of bound water decreases for the halogenated resins, showing that these groups appear to be impeding the water molecules binding to the hydroxyl groups. Correspondingly there is an increase in the free water in the halogenated systems, possibly reflecting more free volume in these systems. By plotting the increment in weight gain against the increment in

dielectric permittivity (Figure 6), two regions are observed. The first slope is the addition of bound water to the resin and the second reflects the redistribution of water into voids and its appearance as free water.

The dielectric results for the DGA based system showed no significant difference in the total amount of water adsorbed in the system although, as with the other system, there was a reduction in the bound water and an increase in the free water (Table 5). In the high frequency

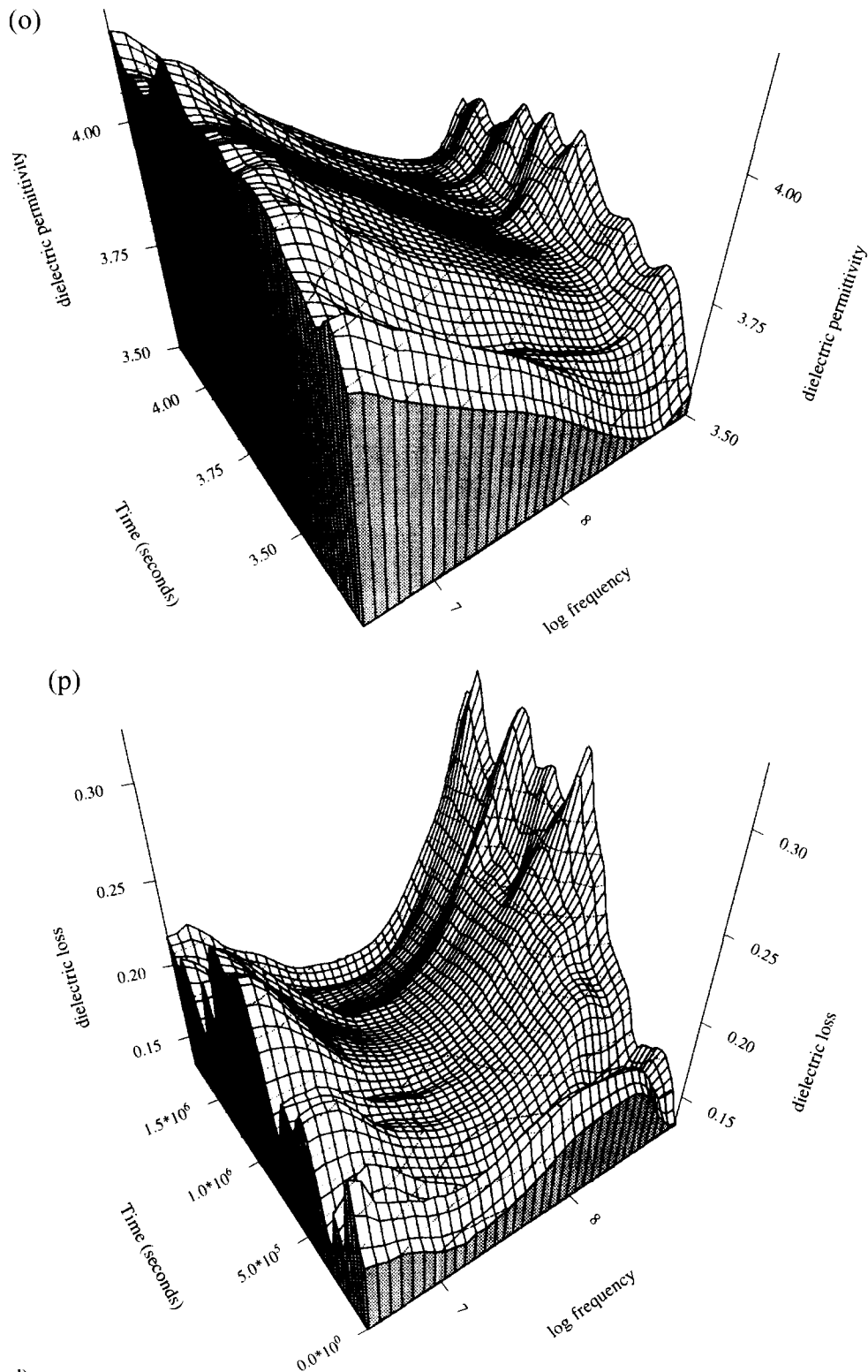


Figure 4 (Continued)

dielectric spectrum water absorption study of the DGA resin cured with *m*-DAB there is surprisingly observed a reduction of the dielectric permittivity with time. The total dielectric increment measured at 10 Hz shows the usually continuous increase, and the observed effects can be attributed to collapse of the microvoids, causing free water to become distributed as bound water. This is reflected by a shift to lower frequency of the dielectric loss peak consistent with an increasing interaction of water molecules with the matrix as time progresses. The

sample was then dried and the experiment repeated. It is well known that in thermoset resins the second absorption of water does not always follow the curve for the first.

The repeat hydration experiments (Figures 4o–4r) do not exhibit the kinetic changes observed in the initial study and indicate that the matrix has now reached a lower equilibrium state. The dielectric loss at high frequency is lower in the rehydration experiment than in the original investigation, and shifts in the loss to lower frequency

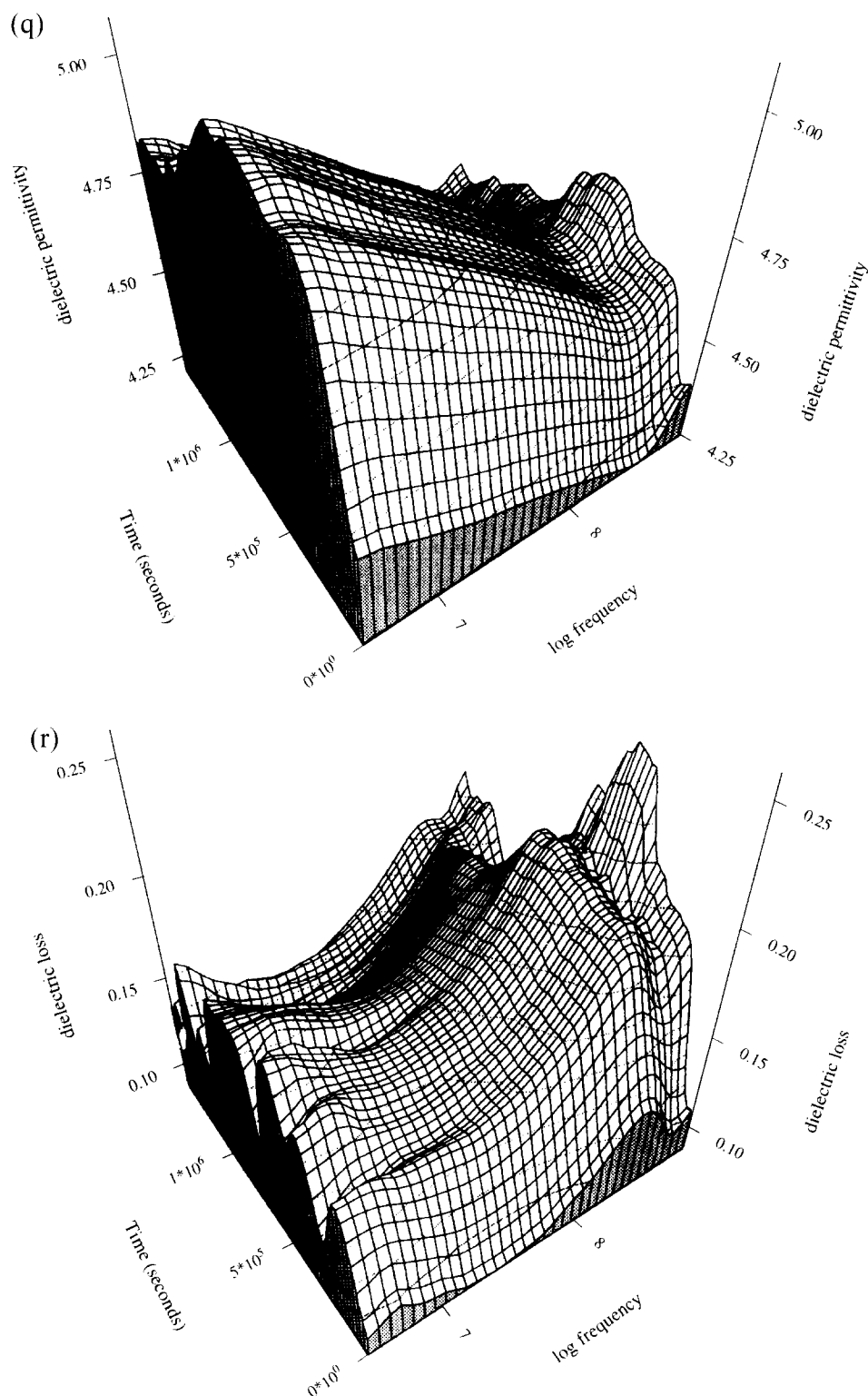


Figure 4 (Continued)

with time were not detected. A possible explanation is that the water absorbed in the initial experiment plasticizes the matrix in the region of the microvoids and allows subsequent rearrangement of the matrix. The water molecules originally in the voids become dispersed as molecular entities in the matrix and behave as bound water. The voids having collapsed are not reformed on drying and hence do not contribute to the subsequent rehydration behaviour, as illustrated in Figure 4k. This is the first case of this phenomenon being observed and

indicates an important relaxation mechanism for the stress stored within thermoset systems on exposure to moisture.

The mechanism for the formation of the microscopic voids into which water segregates is at present unknown; however, it is probably related to the topographical constraints imposed by forming the structure at elevated temperature and then cooling to room temperature. Minimization of the energy will lead to cavity formation in lightly cross-linked areas between highly cross-linked

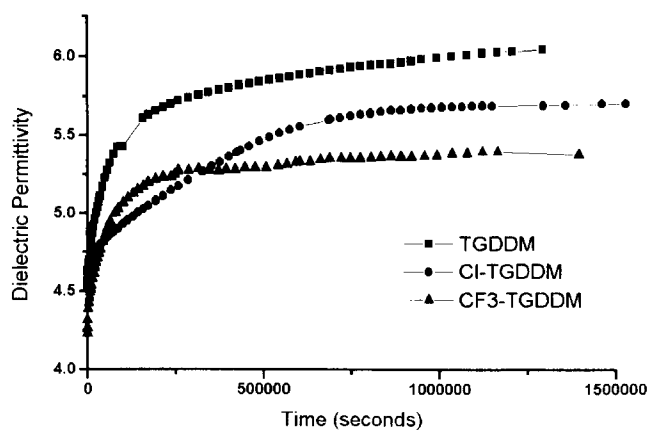


Figure 5 Dielectric diffusion data at 10 Hz for DDS cured system

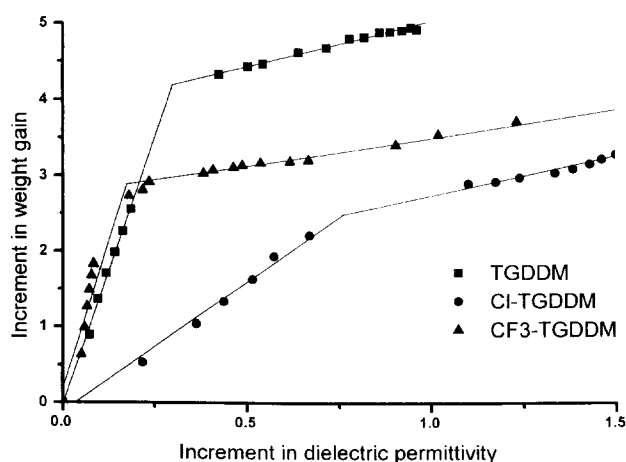


Figure 6 Increment in weight gain as a function of increment in dielectric permittivity

regions. A spherical structure is to be expected as this will represent a minimum energy situation. The size of these micro-voids should be three or six repeat units in diameter and hence would not significantly influence the free volume distribution²⁰. The minimum size of void for free water to exist, which consists of ~ 60 water molecules is $\sim 50 \text{ \AA}$ ³⁷. No attempt has been made in this study to image the size of the voids. The presence of such voids has been previously inferred from the changes in density which occur on cure, and their number and size change as the cure process proceeds. In the fluorinated resins the polymer-polymer interactions are sufficiently different from those of the protonated analogues to alter significantly the number of microscopic voids formed and this is reflected in the distribution of free to bound water in these systems.

CONCLUSIONS

The cure data suggest that there is an enhancement of cure in the TGDDM/DDS system with the incorporation of halogenated substituents into the epoxy ring system. However, in the parallel study of HPT1062 as the curing agent the reverse is observed. There is no obvious reason for these trends. It is possible to speculate that the effect is associated with the formation of an 'activated' complex which allows inductive effects to enhance the opening of

the oxirane ring. Further studies would be required to clarify the nature of these effects. I.r. measurements showed that the cure of the sample was not complete until the sample had been heated to a temperature of about 433 K for these systems. The dielectric study is in agreement with gravimetric data that halogen substitution into an epoxy system has the effect of reducing the amount of water sorption in the system, and that chlorinated resins reduce and trifluoromethyl increases the rate of water sorption. However, for the chlorinated system the equilibrium water content from dielectric data was higher than expected, which could be due to the presence of a porous structure next to the electrode. Analysis of the bound and free water in the systems showed that the incorporation of halogens reduces the amount of bound water in the systems and increases the amount of free water. The first observations of collapse of microvoids are reported and these provide an important mechanism for stress relaxation in resins on absorption of moisture.

ACKNOWLEDGEMENTS

Two of us (E.A.P. and E.H.) wish to thank the Ministry of Defence for EMR studentships for the period of the study. The support of the SRC and EPSRC for D.H. and I. McE. for part of this study is also gratefully acknowledged.

REFERENCES

- 1 Wright, W. W. *Composites* 1981, **12**, 201
- 2 Antoon, M. K., Koenig, J. L. and Serafini, T. *J. Polym. Sci.: Polym. Phys. Edn* 1981, **19**, 1567
- 3 Levy, R. L., Fanter, D. L. and Summers, C. J. *J. Appl. Polym. Sci.* 1979, **24**, 1643
- 4 Williams, J. G. and Delatycki, O. *J. Polym. Sci. A-2* 1970, **8**, 295
- 5 Fuller, R. T., Fornes, R. E. and Memory, J. D. *J. Appl. Polym. Sci.* 1979, **23**, 1388
- 6 Lawing, D., Fornes, R. E., Gilbert, R. D. and Memory, J. D. *J. Appl. Phys.* 1981, **52**, 5906
- 7 Maxwell, I. D. and Pethrick, R. A. *J. Appl. Polym. Sci.* 1983, **28**, 2363
- 8 Netravali, A. N., Fornes, R. E., Gilbert, R. D. and Memory, J. D. *J. Appl. Polym. Sci.* 1984, **29**, 311
- 9 Busso, C. J., Newey, H. A. and Holler, H. V. AFML-TR-69-328, 1970
- 10 Newey, H. A. *US Patent* 3 449 375
- 11 Griffith, J. R. *Chemtech* 1982, 290
- 12 Goobich, J. and Marom, G. *Polym. Eng. Sci.* 1982, **22**, 1052
- 13 Sasaki, S. and Nakamura, K. *J. Polym. Sci.: Polym. Chem. Edn* 1984, **22**, 831
- 14 Johncock, P. and Tudgey, G. F. *Br. Polym. J.* 1983, **15**, 14
- 15 Urbanski, J., Czerwinski, W., Janicka, F., Majewska, F. and Zowell, H. 'Handbook of Analysis of Synthetic Polymers and Plastics', 1 Edn, Ellis Horwood, Chichester, UK, 1977, p. 305
- 16 Haydn, J. and Balzejak, M. *German Patent Specification* 1 206 915, 1965
- 17 Herbert, A. *US Patent* 3 449 375, 1969
- 18 Hayward, D., Gawayne, M., Mahboubian-Jones, B. and Pethrick, R. A. *J. Phys. E: Sci. Instrum.* 1984, **17**, 683
- 19 Kranbuehl, D. 'Developments in Reinforced Plastics', Vol. 5, Elsevier Applied Science, New York, 1986, pp. 181-204
- 20 Kranbuehl, D. in 'Encyclopedia of Composites' (Ed. S. M. Lee), VCH, New York, 1989, pp. 531-543
- 21 Kranbuehl, D., Kingsley, P., Hart, S., Hasko, G., Dexter, B. and Loos, A. C. *Polym. Compos.* 1994, **15**, 297
- 22 Johari, G. and Mangion, M. B. M. *J. Polym. Sci. (B)* 1991, **29**, 1117
- 23 Johari, G. and Mangion, M. B. M. *Macromolecules* 1990, **23**, 3687

- 24 MacDonald, J. R. *Phys. Rev.* 1953, **92**, 4
- 25 Jeffrey, K. and Pethrick, R. A. *Eur. Polym. J.* 1994, **30**, 152
- 26 Mikols, W. J., Seferis, J. C., Apicella, A. and Nicolais, L. *Polym. Compos.* 1982, **3**, 118
- 27 Apicella, A., Egiziano, L., Nicolais, L. and Tucci, V. *J. Mater. Sci.* 1988, **23**, 729
- 28 Crank, J. J. 'The Mathematics of Diffusion', Clarendon Press, Oxford, UK, 1975
- 29 Fujita, H. in 'Diffusion in Polymers' (Eds J. J. Crank and G. S. Park), Academic Press, London, 1968, Ch. 3
- 30 Johncock, P. *Br. Polym. J.* 1986, **18**, 292
- 31 Johncock, P. *J. Appl. Polym. Sci.* 1990, **41**, 613
- 32 Aldrich, P. D., Thurow, S. K., McKennon and Lyssy, M. E. *Polymer* 1989, **28**, 2289
- 33 Pathmanathan, K. and Johari, G. P. *Polymer* 1988, **29**, 303
- 34 Maxwell, I. D. and Pethrick, R. A. *J. Appl. Polym. Sci.* 1983, **28**, 2363
- 35 Maffezzoli, A. M., Peterson, L., Seferis, J. C., Kenney, J. and Nicolis, L. *Polym. Eng. Sci.* 1993, **33**, 75
- 36 Pethrick, R. A., Hollins, E. A., McEwan, I., MacKinnon, A. J., Hayward, D. and Cannon, L. *Macromolecules* 1996, **29**, 5208
- 37 Hasted, J. B. 'Aqueous Dielectrics', Halsted Press, New York, 1973